

A simple mechanism for stable oscillations in the large-scale ocean circulation

Andrew Keane^{1*}, Alexandre Pohl^{2,3}, Henk A. Dijkstra⁴ and Andy Ridgwell³

¹School of Mathematical Sciences and Environmental Research Institute, University College Cork, Cork, Ireland.

²Biogéosciences, UMR 6282, UBFC/CNRS, Université Bourgogne Franche-Comté, 6 boulevard Gabriel, Dijon, F-21000 France.

³Department of Earth and Planetary Sciences, University of California, Riverside, CA, USA.

⁴Institute for Marine and Atmospheric Research Utrecht and Center for Complex Systems Studies, Department of Physics, Utrecht University, Utrecht, the Netherlands.

*Corresponding author(s). E-mail(s): andrew.keane@ucc.ie;

Abstract

The global ocean circulation plays a pivotal role in the regulation of the Earth's climate. The specific pattern and strength of circulation also determines how carbon and nutrients are cycled and via the resulting distribution of dissolved oxygen, where habitats suitable for marine animals occur. However, evidence from both geological data and models suggests that state transitions in circulation patterns have occurred in the past. Understanding the controls on marine environmental conditions and biological productivity then requires a full appreciation of the nature and drivers of such transitions. Here we present an analysis of stable millennial oscillations that occur in the ocean circulation of an Earth System Model of intermediate complexity in the presence of a circumpolar current. To demonstrate that a circumpolar current can act as a driver of stable oscillations, we adapt a simple ocean box model to include a delayed feedback to represent a circumpolar current and investigate the stable millennial oscillatory solutions that arise in the box model by bifurcation analysis. Our results provide new insights into the nature of oscillations that could have occurred under certain continental configurations in the geological past, and also highlight the potential influence of changing circumpolar current speed on the stability of the ocean's meridional overturning circulation.

Keywords: Delay dynamics, Oscillation, Ocean circulation, Bifurcation

1 Introduction

The ocean circulation plays a critical role in the Earth's global climate system. Wind-driven currents acting over the first hundreds of meters impose the first-order pattern and magnitude of

ocean heat transport, and therefore largely determine superficial climate and notably the latitudinal gradient of temperature [1]. Upper-ocean currents also control equatorial and coastal upwelling position and strength, thus the spatial patterns of primary productivity and extension of

oxygen minimum zones [2]. Density-driven deep-ocean circulation, on the other hand, drives ocean mixing, the redistribution of nutrients in the global ocean (and critically, their return back to the ocean surface) [3] as well as the sequestration of atmospheric carbon in the ocean interior [4]. Overturning circulation also controls the transport of oxygen equilibrated in surface seawater into the ocean interior (‘ventilation’) and, ultimately, the capacity of the ocean to host animal life at depth [5, 6].

Abundant sedimentological, geochemical, and paleontological data demonstrate that the global ocean circulation has significantly varied through geological time. At the (multi-)million-year scale, it varied in response to continental rearrangement. For instance, Trabucho Alexandre et al. [7] propose that intense deoxygenation and the deposition of organic-rich sediments developed in the mid-Cretaceous North Atlantic as a consequence of a specific ocean circulation pattern making this ocean basin act as a nutrient trap. A similar mechanism was suggested by Meyer et al. [8] to explain photic-zone euxinia expansion in the Paleo-Tethys ocean at the Permian-Triassic boundary. At a higher frequency, the ocean circulation, both shallow and deep, is also known to vary in concert with global climate. Today, vigorous deep-water formation takes place in the North Atlantic (and Southern) ocean while limited ventilation is observed at similar northern latitudes in the Pacific [9]. During the Last Glacial Maximum, sediment core proxy data for ocean ventilation suggest that the North Pacific was better ventilated at intermediate depths [9], while the Atlantic circulation was probably more sluggish (shallower and/or less vigorous) [10]. Similarly, Freeman et al. [9] used radiocarbon measurements to reconstruct the benthic–planktonic ^{14}C age offset (i.e. ‘ventilation age’) during the last deglaciation and demonstrated a seesaw in the ventilation of the intermediate Atlantic and Pacific Oceans.

In order to assimilate the proxy database in a quantitative framework and gain mechanistic understanding of the drivers of observed changes in ocean properties, (paleo)climatologists use ocean-atmosphere general circulation models (GCMs) [11–13]. These models provide complex representations of ocean physics and dynamics and the coupling with the atmospheric component, sea ice, and possibly ocean biogeochemistry

and land surface [14]. Models of the Coupled Model Intercomparison Project phase 6 (CMIP6), for instance, aim to offer a satisfactory representation of the climate system [15]. However, these models are computationally expensive and consequently, are generally run only for a few hundred to a thousand years. Because this duration approaches the ocean mixing timescale, it is assumed that it allows the model to approximately reach deep-ocean equilibrium, i.e., the physical characteristics of the whole ocean (temperature and salinity), and thus ocean dynamics, are supposed stable from that point in time [11, 16]. By doing so, it is also implicitly assumed that the ocean circulation does in fact eventually reach a stable steady state. Yet, various attempts to run global climate models for a longer time period demonstrated more complex behaviors of the ocean circulation, which sometimes exhibits regimes of stable oscillations. Oscillations have notably been simulated in ocean-only GCMs [17, 18] and ocean GCMs coupled to simple atmospheric components (Earth system Models of Intermediate Complexity; EMICs) [19, 20]. To our knowledge, the only studies reporting such oscillations based on ocean-atmosphere GCM simulations are Refs. [21, 22] using the fully coupled HadCM3 GCM, and the last glacial CESM simulations of Vettoretti et al. [23]. The absence of further documentation of stable oscillatory regimes in other fully coupled GCMs is not surprising considering that a simulation duration of at least 6 thousand years seems to be required to identify stable oscillations, while a typical run-time for GCMs used to explore past (geological) climate states is typically only ca. 3 thousand years (e.g. [13, 24, 25]).

The existence of regimes of stable oscillations in ocean circulation has recently been demonstrated by Pohl et al. [3] for specific combinations of past continental configuration and climatic state. The oscillations have been invoked to explain both the poorly-oxygenated oceans that pervaded several hundreds of millions of years ago [26], when marine life started diversifying in the marine realm [27], as well as enigmatic thousand-year scale cycles identified in marine sediments of the deep geological past [28]. Based on recent studies that pinpoint the tight coupling between marine redox conditions and marine biodiversity

[6, 29–31], the authors conclude that the simulated high-frequency variability in ocean redox conditions would have constituted harsh conditions for the development of marine life at that time. This study exemplifies the implications that such oscillations have for our understanding of the evolution of both global climate and marine biodiversity, but also highlights the need to better characterize the physical mechanisms causing these oscillations. Pohl et al. [3] focused on the consequences of the resulting state transitions in ocean circulation for ocean oxygenation and the interpretation of geological redox indicators, rather than on the underlying mechanisms of the oscillations. In addition, the experimental setup used by the authors, involving complex land mass shapes and configurations, as well as the presence in the model of a variety of climatic and biogeochemical feedbacks, creates challenges for detailed analysis. As a result, the physical mechanisms causing the stable oscillations and state transitions in ocean dynamics in cGENIE remain to be fully elucidated.

Here, we analyse the mechanisms at play by combining a series of new Earth system model experiments conducted using an idealised ocean configuration, with a box model designed specifically to reproduce and identify key characteristics of the cGENIE simulations. Experiments with the idealised continental configuration serve as a stepping-stone between results of oscillations in simulations using “real-world” continental configurations [3] and understanding gained through the analysis of simple ocean box models.

Box models have been often used to identify physical mechanisms of oscillatory behavior in the ocean-climate system. Regarding variability of the meridional overturning circulation, two basic types of oscillatory behavior have been identified. Overturning (or loop) oscillations can be found in a four-box model [32] and involve the advective propagation of a buoyancy anomaly along the overturning loop. Such variability is of centennial time scale when only the Atlantic is considered and millennial scale when the global overturning is considered [18]. Oscillatory variability may also be induced by convective processes. The basics of the behavior can be understood from the so-called ‘flip-flop’ oscillation [33],

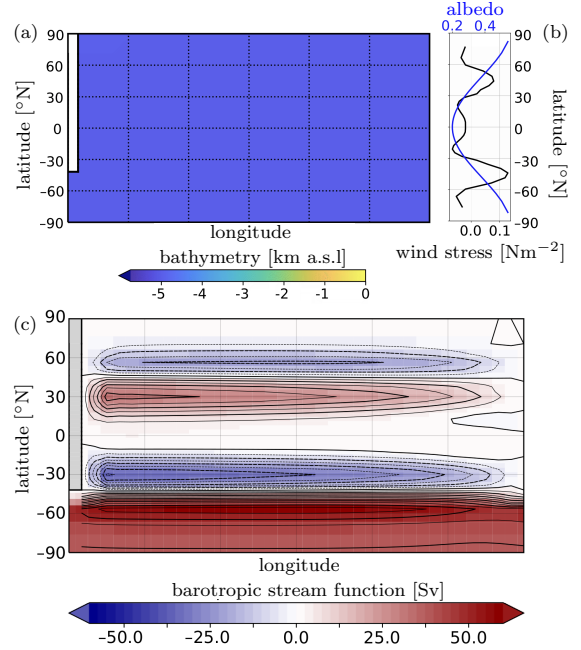


Fig. 1 cGENIE Drake World setup. (a) Model bathymetry. Landmasses (above sea level; a.s.l.) are shaded white. (b) Zonal wind stress and zonal albedo fields used as boundary conditions. (c) Barotropic streamfunction (Sverdrup, $1 \text{ Sv} = 10^6 \text{ m}^3 \text{ s}^{-1}$) simulated at $\times 16$ CO₂ (\times CO₂, the pre-industrial atmospheric concentration of 280 ppm). The boundary is periodic in the horizontal direction.

where oscillations between convective and non-convective states occur. The origin of the millennial time-scale oscillations, also referred to as ‘deep-decoupling’ oscillations or ‘flushes’ is, however, in more detailed models best explained by a box model which combines both advective and convective processes [34].

Here, we present a model that reproduces the oscillations obtained in the cGENIE Earth system model [3] in a very simple way, by embedding key climatic features in a simple 3-box model. The novel element is that a time delay is introduced, which serves as an efficient representation of the effects of a circumpolar current on the oceanic salt transport.

2 EMIC experiments

To gain insight into the existence of self-sustained oscillations in the ocean circulation, numerical simulations are conducted using an idealized setup of the EMIC cGENIE [35]. cGENIE consists of a reduced physics (frictional geostrophic)

3D ocean circulation model coupled to a 2D energy-moisture-balance atmospheric component plus sea-ice module. (Although we do not show the results of it here, cGENIE also includes a state-of-the-art representation of marine biogeochemistry e.g. [35].) Compared to CMIP6 Earth System models, the simplified climatic component of cGENIE offers a rapid model integration time, permitting the model to be run for tens of thousands of years.

The adopted idealized cGENIE setup is “Drake World”. This differs slightly from the classic MIT GCM implementation [36] and rather than a purely numerical barrier to flow, is characterized by a thin strip of land extending southwards to 45°S and a 5-km deep flat-bottomed ocean everywhere else. The model uses a 36×36 equal-area horizontal grid, with 16 unevenly-spaced z -coordinate vertical levels in the ocean (Fig. 1(a)). We apply idealized boundary conditions of zonally averaged wind stress and speed, plus a zonally averaged planetary albedo, following Vervoort et al. [37] and van de Velde et al. [38] (Fig. 1(b)). The solar constant is set to modern (1368 W m^{-2}). The physical parameters controlling the model climatology follow Cao et al. [39]. Additional experiments are conducted using an alternative, idealized continental configuration with a strip of land extending from the North Pole to the South Pole (“Ridge World” [3, 36]) and everything else unchanged.

Figure 1(c) shows the barotropic stream-function (units of Sverdrup, $1 \text{ Sv} = 10^6 \text{ m}^{-3} \text{ s}^{-1}$), as a measure of the vertically averaged flow, in Drake World at $\times 16 \text{ CO}_2$ ($\times \text{CO}_2$, the pre-industrial atmospheric concentration of 280 ppm). As with all the following results, this shows the state of the model following spin-up (i.e. after all transient behaviour has died away). The most notable feature of the barotropic stream-function is the strong zonal flow in the southern channel, similar to the Antarctic Circumpolar Current observed in the Earth’s modern continental configuration. It is a mainly wind-driven current that constantly transports water around the pole and persists also for the other values of pCO_2 considered here.

We find that when atmospheric forcing is varied in the model (from $\times 4 \text{ CO}_2$ to $\times 16 \text{ CO}_2$), ocean dynamics exhibits a complex response. Overall, we observe a gradual shift in the locus

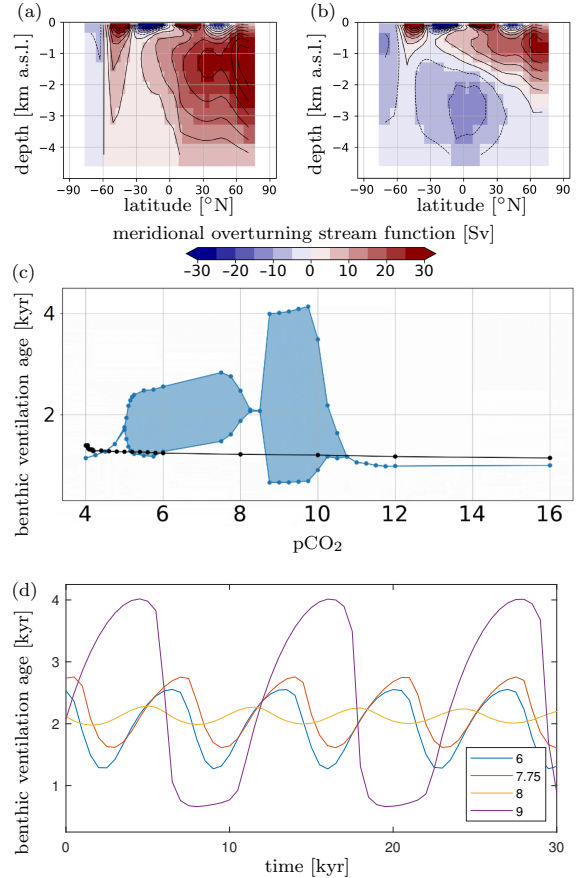


Fig. 2 cGENIE results. Meridional overturning stream-function for Drake World at (a) $\times 4 \text{ CO}_2$ and (b) $\times 16 \text{ CO}_2$. (c) Envelope of benthic ventilation ages (i.e. annual global mean time since water at the deepest depth level was last at the surface) simulated at various atmospheric CO_2 levels, illustrating regimes of stable equilibria (where no envelope is visible) and stable oscillations (where the envelope can be seen), for Drake World (blue) and Ridge World (black). (d) Example time series of stable oscillations (legend indicates $\times \text{CO}_2$) simulated using Drake World with transients (initial spin-up of 30 kyr) removed.

of deep-water formation from the (oceanic) North Pole (Fig. 2(a)) to the South Pole (Fig. 2(b)). Interestingly, during this shift we encounter two families of stable oscillations.

The blue points in Fig. 2(c) show the annual global mean benthic ventilation age (i.e. time length since water in the deepest ocean level was at the surface level) for an ensemble of simulations in Drake World. Because the simulations take a long time to run (around 6 days for a 60-kyr long cGENIE simulation as shown in Fig. 2(c)), they are run in parallel for different pCO_2 levels using the same initial conditions. As pCO_2 increases,

the ocean transitions from a stable steady state with northern deep-water formation to a regime of stable oscillations between northern deep-water formation and a weakened circulation state (represented by the envelopes in Fig. 2(c)). This weakened state becomes stable near $\times 8.5 \text{ CO}_2$. Further increasing of pCO_2 gives rise to another regime of stable oscillations between a largely collapsed circulation state and strong circulation with southern deep-water formation. Finally, the southern deep-water formation steady state becomes stable for large values of pCO_2 . Example time series of the oscillations are shown in Fig. 2(d).

An additional series of experiments conducted on Ridge World, i.e., under identical boundary conditions but with the strip of land extending to the southernmost grid points, do not exhibit regimes of stable oscillations (black points in Fig. 2(c)), at least not for the values of pCO_2 tested. A primary question addressed in this paper is then: Why do these oscillations appear once the ocean has an open-ocean passage around the South Pole?

3 Simple box model

We begin with the simplified ocean box model from Ref. [40], which consists of two polar boxes and one upper equatorial box (Fig. 3). Assuming salt conservation, the model is written in terms of the salt content of the two polar boxes. We adapt the model to include the effect of zonal transport in the southern channel by including a delayed feedback term on the salinity of box 1. In particular, a parcel of water in the southern polar box will leave its position at time t and return to the same position at time $t + \tau$. The model becomes a set of delay differential equations for the salinity variables $S_{i \in \{1,2\}}$:

$$\begin{aligned} V \dot{S}_1 &= S_0 F_1 + m (S_2 - S_1) + \sigma (S_1^\tau - S_1) \quad (1) \\ V \dot{S}_2 &= -S_0 F_2 + m (S_3 - S_2). \end{aligned}$$

Parameters F_1 and F_2 represent surface freshwater fluxes between the boxes. The delayed variable $S_1^\tau = S_1(t - \tau)$ has delay time τ and σ is the feedback strength. The variable m represents the volume transport between boxes due to the

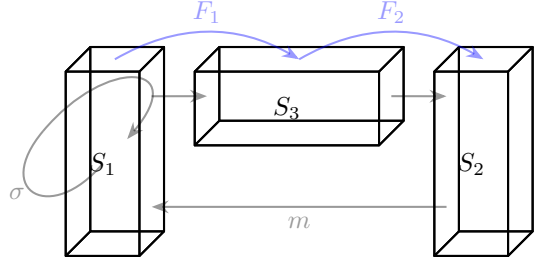


Fig. 3 Boxes representing regions of the ocean with salinity variables $S_{i \in \{1,2,3\}}$ with arrows representing meridional water flux of strength m and zonal flux of strength σ . Parameters F_1 and F_2 represent freshwater fluxes.

density gradient across the ocean:

$$m = k [\beta (S_2 - S_1) - \alpha T^*]. \quad (2)$$

Parameter k is a hydraulic constant, while β and α are salinity and temperature expansion coefficients, respectively. The model assumes a fixed temperature gradient T^* between the northern and southern boxes. Assuming that salt is conserved, we have $S_3 = 3S_0 - S_1 - S_2$. Parameter V is the (equal) volume of the boxes and S_0 is a reference salinity. In Fig. 3, a positive m corresponds to clock-wise circulation. Note that here we only discuss the positive m solutions, and therefore omit the negative m equations from the model description.

In this paper we take parameter values from Ref. [40] and let $k = 23 \times 10^{17} \text{ m}^3 \text{ yr}^{-1}$, $\alpha = 1.7 \times 10^{-4} \text{ K}^{-1}$, $\beta = 0.8 \times 10^{-3} \text{ psu}^{-1}$, and $S_0 = 35 \text{ psu}$. We let $V = 3.5 \times 10^{17} \text{ m}^3$, which is approximately the volume of the southern channel in Drake World. Furthermore, we set $F_2 = 1 \text{ Sv}$ ($10^6 \text{ m}^3 \text{ s}^{-1}$) and $T^* = 0 \text{ K}$, and note that qualitatively similar results to those presented below are found when varying these parameters. Finally, we approximate delay times for each latitude within the southern channel using averaged zonal ocean speeds from cGENIE simulations across longitude and depth. The average of these delay times gives us a rough estimate for τ of about 1000 years. Therefore, we use similar values for τ in the results presented below.

Clearly, the box model representation is very much highly simplified compared to a dynamic 3D ocean circulation model. As such, we do not attempt to find quantitative agreement between the two models. Rather, we demonstrate that this

simple model possesses surprisingly rich dynamics and is sufficient for a qualitative reproduction of the interesting ocean circulation behaviour observed in cGENIE experiments.

In Ref. [40] the model without the delayed feedback was shown to exhibit, not only the typical bistability between upper ($m > 0$) and lower ($m < 0$) branches of solutions, but also a Bogdanov-Takens bifurcation. This means that instead of the upper branch losing stability at a fold bifurcation, it may for certain values of freshwater flux already lose stability at a Hopf bifurcation, which is always subcritical [41]. The resulting unstable periodic orbits terminate at homoclinic bifurcations.

In the following section, solutions to model (1) and their stability properties are found using the numerical continuation package DDE-Biftool [42–45].

4 Stable oscillations

The solutions to the box model shown in Fig. 4 demonstrate how the delayed-feedback effect allows the existence of stable periodic orbits. Black curves show the steady-state solutions of S_1 as parameter F_1 is varied, while the blue curves indicate the maximum of S_1 for periodic solutions. Solid and dashed curves indicate stable and unstable solutions, respectively. In panel (a) the parameter σ is set to zero; that is, there is no delayed-feedback effect. In this case, as F_1 increases, the stable steady-state solution loses stability at a subcritical Hopf bifurcation, resulting in a branch of unstable periodic orbits. When the delayed feedback is active, the Hopf bifurcation may become supercritical, resulting in a branch of stable periodic orbits, as shown in panel (b). In this particular example, the stable periodic solutions lose stability at a torus bifurcation before encountering a fold of periodic orbits. The periods of the resulting stable oscillations have a millennial timescale as demonstrated by the example time series shown in panel (c).

Some readers familiar with control theory may not be surprised by the ability of the delayed feedback to stabilize the pre-existing periodic orbits. Pyragas control takes the same mathematical form as the additional term in our model that represents the zonal flow. It is used to stabilize unstable periodic orbits, as has been demonstrated in many

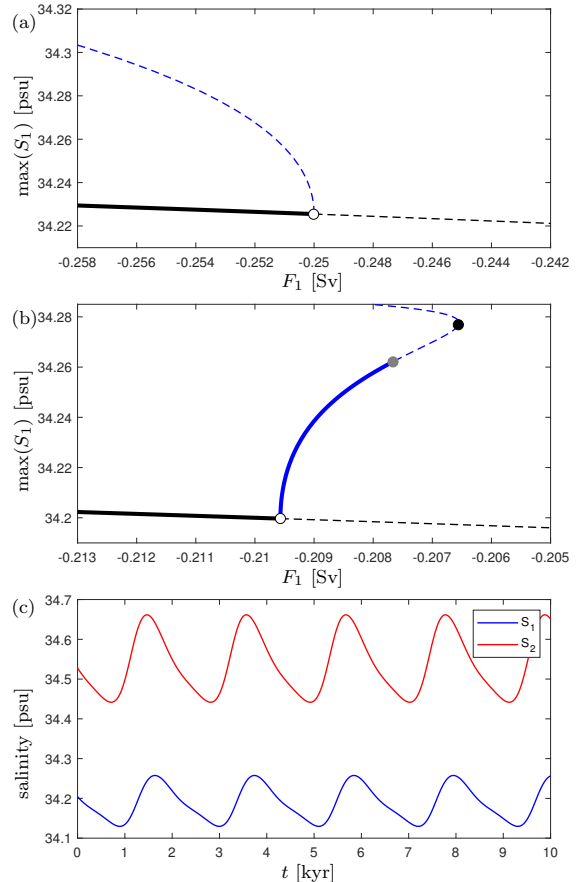


Fig. 4 Solutions of model (1) depending on freshwater forcing parameter F_1 . Solid/dashed curves represent stable/unstable solutions. Black are equilibria and blue are maxima of periodic solutions. White, gray, and black filled circles represent Hopf, torus, and fold bifurcations, respectively. (a) is without the delayed feedback (i.e. $\sigma = 0$), while (b) is with $\sigma = 11$ Sv. The delay time τ is set to 900 years. (c) shows an example time series with $\sigma = 11$ Sv and $F_1 = -0.208$ Sv.

applications, for example, in semiconductor laser experiments [46, 47]. To be precise, the delayed feedback effect in our model is not equivalent to Pyragas control. In the latter, the control is applied to all variables of the system (we only apply it to the salinity in one box) and the delay time is set equal to the period of the unstable periodic orbit to be stabilised. Nonetheless, the method may still be successful for other delay times, as investigated in Ref. [48]. In model (1) we find that the periods of the stable oscillations are generally at least twice the delay time.

Whether the delayed feedback induces a change in criticality of the Hopf bifurcation

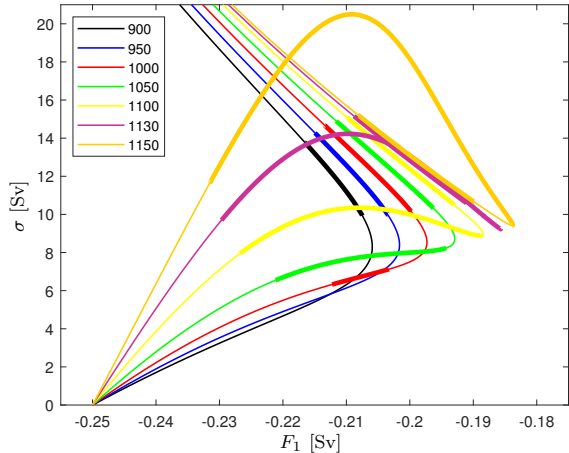


Fig. 5 Curves of Hopf bifurcations. At a Hopf bifurcation the steady-state solution loses (or gains) stability and produces a branch of periodic solutions. Where the curves are thin/thick the Hopf bifurcation produces a branch of unstable/stable periodic solutions. The colours refer to different delay times τ shown in the legend.

depends on the feedback parameters σ and τ . Figure 5 illustrates this dependence, where curves of Hopf bifurcations are calculated in the (F_1, σ) -plane for different values of τ . The thick parts of the curves indicate that the Hopf bifurcation is supercritical. Notice that, depending on the feedback strength and delay time, it is possible that the system experiences multiple Hopf bifurcations as F_1 increases.

Figure 6(a) is a bifurcation diagram showing the amplitude of oscillations in terms of mean benthic ventilation age constructed from simulation results of cGENIE using Drake World. We observe that as $p\text{CO}_2$ is increased the steady-state solution loses stability near $\times 5$ $p\text{CO}_2$. The amplitude growth near this bifurcation point resembles a square-root law, typical of a Hopf bifurcation [49]. The family of periodic solutions disappears at, what appears to be, another supercritical Hopf bifurcation near $\times 8$ $p\text{CO}_2$. The bifurcation point must be very close to $\times 8$ $p\text{CO}_2$, since it was necessary to run the simulation for an extremely long time (up to 120 thousand years) while the amplitude of the oscillations continued to decrease very slowly. Finally, the steady-state solution again loses stability after $\times 8.5$ $p\text{CO}_2$.

As illustrated in Fig. 5 we may choose parameter values so that the system will pass through two supercritical Hopf bifurcations as F_1 increases. Realistically, F_1 is not the only parameter value

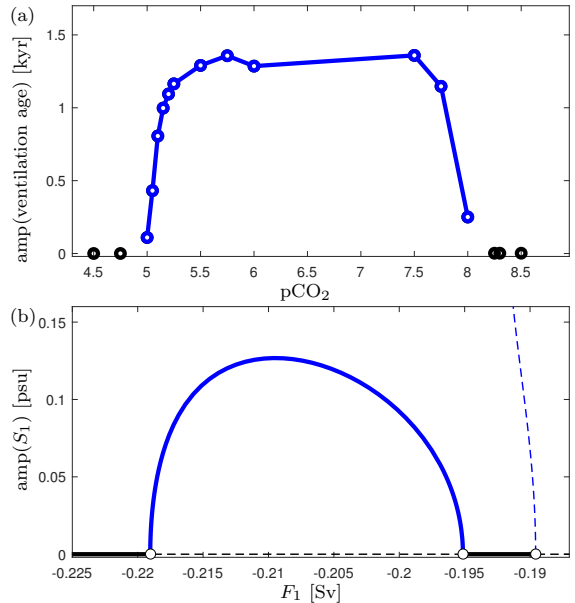


Fig. 6 Amplitudes of oscillations with steady-state and periodic solutions shown in black and blue, respectively. (a) cGENIE experiments with varying $p\text{CO}_2$. (b) Model (1) solutions while varying F_1 with $\sigma = 9.5$ Sv and $\tau = 1100$ years. White filled circles represent Hopf bifurcations.

that would change due to changes in $p\text{CO}_2$. Parameters F_2 , T^* , σ and τ would all be susceptible to influence from atmospheric changes. Nonetheless, we only consider varying F_1 in an effort to keep the analysis simple and demonstrate qualitative changes in behaviour. Figure 6(b) shows that the effect of the circumpolar current is sufficient for reproducing a family of periodic solutions between two supercritical Hopf bifurcations. In the box model the steady-state solution finally loses stability at a subcritical Hopf bifurcation.

Figure 7(a) is the same as Fig. 6(a), only for higher $p\text{CO}_2$. Near $\times 8.5$ $p\text{CO}_2$ we observe a jump to large-amplitude oscillations, as well as bistability between steady-state and oscillatory solutions. Both the jump to large-amplitude oscillations and bistability are reproduced by the box model in panel (b). Here, the steady-state solution loses stability in a subcritical Hopf bifurcation. The unstable periodic orbits become stable via a fold bifurcation of periodic orbits, before later losing stability at a torus bifurcation.

The termination of the large-amplitude oscillations in Fig. 7(a) involves co-existing oscillatory solutions at $\times 10.0$ $p\text{CO}_2$ and a gradual transition to a state of strong convection at the southern

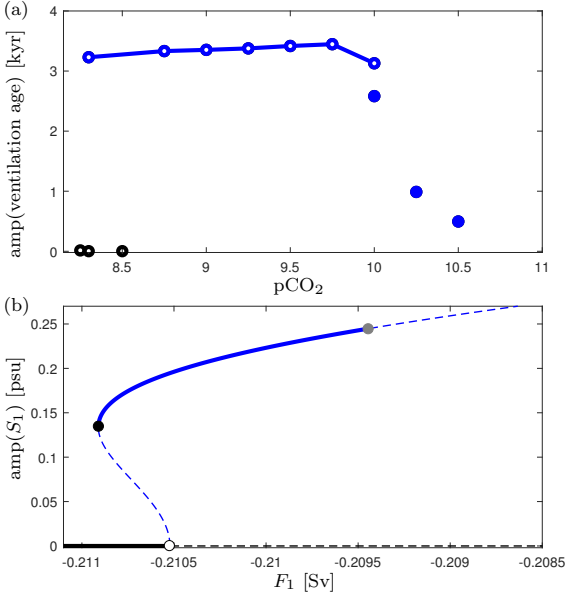


Fig. 7 Amplitudes of oscillations with steady-state and periodic solutions shown in black and blue, respectively. (a) cGENIE experiments with varying $p\text{CO}_2$ with steady-state and periodic solutions shown as black and blue circles, respectively. Filled blue circles indicate solutions not captured by the box model. (b) Model (1) solutions while varying F_1 with $\sigma = 9$ Sv and $\tau = 850$ years. White, black and gray filled circles represent Hopf, fold and torus bifurcations, respectively.

pole. These solutions are shown as filled blue circles in panel (a). Following these oscillatory solutions, for larger values of $p\text{CO}_2$, we only find steady-state solutions that correspond to $m < 0$ solutions in the box model, which we do not consider here for simplicity. The re-creation of transitions between strong and weak convecting states in the box model would require upper and lower boxes, as well as the introduction of an additional convection timescale into the dynamics as in Ref. [34], and is therefore beyond the scope of model (1).

5 Discussion

The delayed feedback provides the simple box model with the capacity to mimic important qualitative behaviour observed in cGENIE experiments using an idealized configuration. It hence provides a simple mechanism for the occurrence of stable oscillations in the ocean circulation and its dependence on a zonal flow across the southern

channel. The analysis, conducted using the numerical continuation software DDE-Biftool, highlights the need for each system parameter to be within a certain range of values in order for oscillations to be observed. For the cGENIE model, this implies that oscillations could easily be missed if, for example, the wind strength over the southern channel is too weak so that the delayed feedback effect is not strong enough.

The results presented here provide an explanation for observations in cGENIE experiments using realistic continental configurations of the geological past, where stable oscillations coincide with configurations having a large open ocean pole [3]. These cGENIE oscillations, which occur on the millennial timescale, could shed light on periods of high variability observed in high-resolution proxy data [28].

Despite some evidence of stable oscillatory behaviour in GCMs [22], the extended run-time of such models makes them ill-suited for the explorations through parameter space required when investigating possible causes and attributing factors of oscillatory behaviour. cGENIE, on the other hand, represents a very practical compromise for establishing connections between interesting dynamics and fundamental mechanisms that drive them. As such, this study is conducted in a similar vein to some previous studies that have conducted parameter sweeps in order to identify possible bifurcations and regions of qualitatively different climate states (for example, see Refs. [50–52]).

The way that the stable oscillations presented here are generated by delayed feedback (in turn, by continental configuration) is different to previous studies of ocean models. In some past studies convection and associated deep-water flushes have been the driving mechanism for oscillations [33, 34]. In other studies sea-ice dynamics are required as part of a feedback mechanism that generates oscillations [53–55]. One logical next step is to investigate how the delayed feedback interacts with these other sources of oscillations. There is evidence from cGENIE simulations (not shown) of quasi-periodic behaviour, which could be the result of an interaction between multiple mechanisms for oscillations.

The simple box model with delayed feedback does not reproduce all dynamical features observed in the cGENIE experiments, such as the

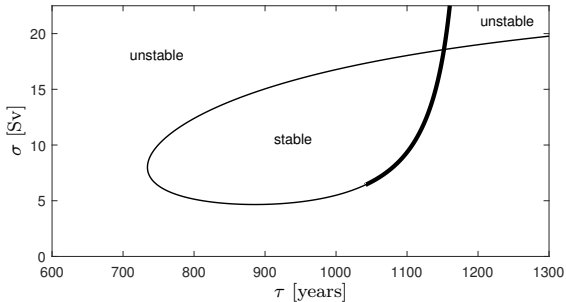


Fig. 8 Stability diagram of the steady-state solution at $F_1 = -0.22$ Sv in the (σ, τ) -plane. Non-bold/bold curves show subcritical/supercritical Hopf bifurcations.

oscillations shown as blue filled circles in Fig. 7. Furthermore, although the simple model captures the millennial timescale of the stable oscillations, the period of the oscillations observed in cGENIE can easily exceed 10 thousand years (for example, the large-amplitude oscillations around $\times 9$ pCO₂ in Fig. 2(c)), which is not found in the simple model. A further modelling possibility that would effect the timescales in the box model includes adding more boxes to the box model. Finally, deep-water flushes could be captured by a salinity delay due to a deep-ocean adjustment to convective events, which would further increase the delay time of the model.

Results of our box model may also have implications for our understanding of future changes in the global ocean circulation. It has been reported that part of the Antarctic Circumpolar Current (ACC) is accelerating due to anthropogenic ocean warming [56]. This would correspond to a shortened delay time in the feedback of model (1). Figure 8 shows a curve of Hopf bifurcations that demonstrates the sensitivity of an example $m > 0$ solution ($F_1 = -0.22$ Sv) to changes in the feedback. Interestingly, it is stable only for intermediate values of feedback strength and delay time. In both scenarios of increasing and decreasing delay time, the steady-state solution loses stability at a Hopf bifurcation. For the parameters used in Fig. 8, there are segments of supercritical Hopf bifurcations (bold), which give rise to stable oscillations, as well as, subcritical Hopf bifurcations (non-bold). The latter corresponds to so-called “dangerous” bifurcation [57], where the system jumps suddenly and irreversibly to a remote state with an alternative circulation pattern. Therefore, the dynamics discussed in this paper could also

be relevant in a modern context. Of course, the Drake Passage of modern continental configuration is smaller than the passage of the Drake World setup used here (Fig. 1(a)). Nonetheless, it is worthwhile to consider the possibility that changes in zonal flow, such as that of the ACC, could play a part in destabilising the meridional overturning circulation of the Atlantic Ocean.

Declarations

Funding

This is a contribution of UMR 6282 Biogeosciences Team SEDS. The project has received funding from the Netherlands Earth System Science Center (NESSC), OCW grant No. 024.002.001 (HD). AR acknowledges support from NSF grant EAR-2121165, as well as from the Heising-Simons Foundation. This work benefited from a research visit of AK to University of California-Riverside funded by a Charlemont grant from the Royal Irish Academy.

Competing Interests

The authors have no relevant financial or non-financial interests to disclose.

Author Contributions

Mathematical modelling was completed by A.K. and H.D. A.K. conducted the bifurcation analysis. A.P. and A.R. conducted the cGENIE experiments and analysis of the results. All authors contributed to writing the manuscript and approved the final version.

Code availability

The code for the version of the muffin release of the cGENIE Earth system model used in this paper, is tagged as v0.9.32, and is assigned a DOI: 10.5281/zenodo.6987451. Configuration files for the specific experiments presented in the paper can be found in the directory: genie-userconfigs/PUBS/submitted/Keane_et_al.ClimateDynamics. Details of the experiments, plus the command line needed to run each one, are given in the readme.txt file in that directory. All other configuration files and boundary conditions are provided as part of the code release. A manual

detailing code installation, basic model configuration, tutorials covering various aspects of model configuration, experimental design, and output, plus the processing of results, is assigned a DOI: 10.5281/zenodo.5500696.

References

- [1] B.E. Rose, D. Ferreira, Ocean heat transport and water vapor greenhouse in a warm equable climate: A new look at the low gradient paradox. *Journal of Climate* **26**(6), 2117–2136 (2013). <https://doi.org/10.1175/JCLI-D-11-00547.1>
- [2] A. Pohl, D.A.T. Harper, Y. Donnadieu, G. Le Hir, E. Nardin, T. Servais, Possible patterns of marine primary productivity during the Great Ordovician Biodiversification Event. *Lethaia* **5**(2), 187–197 (2017). URL <http://doi.wiley.com/10.1111/let.12247>
- [3] A. Pohl, A. Ridgwell, R.G. Stockey, C. Thomazo, A. Keane, E. Vennin, C.R. Scotese, Continental configuration controls ocean oxygenation during the Phanerozoic. *Nature* **608**(7923), 523–527 (2022)
- [4] N. Bouttes, D. Paillard, D.M. Roche, Impact of brine-induced stratification on the glacial carbon cycle. *Climate of the Past* **6**(5), 575–589 (2010). <https://doi.org/10.5194/cp-6-575-2010>
- [5] A. Pohl, Z. Lu, W. Lu, R.G. Stockey, M. Elrick, M. Li, A. Desrochers, Y. Shen, R. He, S. Finnegan, A. Ridgwell, Vertical decoupling in Late Ordovician anoxia due to reorganization of ocean circulation. *Nature Geoscience* **14**(11) (2021). <https://doi.org/10.1038/s41561-021-00843-9>
- [6] R. Stockey, A. Pohl, A. Ridgwell, S. Finnegan, E.A. Sperling, Decreasing Phanerozoic extinction intensity as a consequence of Earth surface oxygenation and metazoan ecophysiology. *Proceedings of the National Academy of Sciences of the United States of America* **118**(41), e2101900,118 (2021). <https://doi.org/10.1073/pnas.2101900118>
- [7] J. Trabucho Alexandre, E. Tuentner, G.A. Henstra, K.J. Van Der Zwan, R.S. Van De Wal, H.A. Dijkstra, P.L. De Boer, The mid-Cretaceous North Atlantic nutrient trap: Black shales and OAEs. *Paleoceanography* **25**(4), PA4201 (2010). <https://doi.org/10.1029/2010PA001925>
- [8] K.M. Meyer, L.R. Kump, A. Ridgwell, Biogeochemical controls on photic-zone euxinia during the end-Permian mass extinction. *Geology* **36**(9), 747–750 (2008). URL <https://pubs.geoscienceworld.org/geology/article/36/9/747-750/29854papers2://publication/doi/10.1130/G24618A.1>
- [9] J.W. Rae, W.R. Gray, R.C. Wills, I. Eisenman, B. Fitzhugh, M. Fotheringham, E.F. Littley, P.A. Rafter, R. Rees-Owen, A. Ridgwell, B. Taylor, A. Burke, Overturning circulation, nutrient limitation, and warming in the Glacial North Pacific. *Science Advances* **6**(50), eabd1654 (2020). <https://doi.org/10.1126/sciadv.abd1654>
- [10] J.N. Howe, A.M. Piotrowski, T.L. Noble, S. Mulitza, C.M. Chiessi, G. Bayon, North Atlantic Deep Water Production during the Last Glacial Maximum. *Nature Communications* **7**, 1–8 (2016). <https://doi.org/10.1038/ncomms11765>
- [11] Y. Donnadieu, E. Pucéat, M. Moiroud, F. Guillocheau, J.F. Deconinck, A better-ventilated ocean triggered by Late Cretaceous changes in continental configuration. *Nature Communications* **7**, 10,316 (2016). <https://doi.org/10.1038/ncomms10316>
- [12] D. Ferreira, J. Marshall, B. Rose, Climate determinism revisited: Multiple equilibria in a complex climate model. *Journal of Climate* **24**(4), 992–1012 (2011). <https://doi.org/10.1175/2010JCLI3580.1>
- [13] M. Laugié, Y. Donnadieu, J.b. Ladant, L. Bopp, C. Ethé, F. Raison, Exploring the impact of Cenomanian paleogeography and marine gateways on oceanic oxygen. *Paleoceanography and Paleoclimatology* **36**(January), e2020PA004,202 (2021). <https://doi.org/10.1029/2020PA004202>

- [14] P. Sepulchre, A. Caubel, J.B. Ladant, L. Bopp, O. Boucher, P. Braconnot, P. Brockmann, A. Cozic, Y. Donnadieu, V. Estella-Perez, C. Ethé, F. Fluteau, M.A. Foujols, G. Gastineau, J. Ghattas, D. Hauglustaine, F. Hourdin, M. Kageyama, M. Khodri, O. Marti, Y. Meurdesoif, J. Mignot, A.C. Sarr, J. Servonnat, D. Swingedouw, S. Szopa, D. Tardif, IPSL-CM5A2. An Earth System Model designed for multi-millennial climate simulations. *Geoscientific Model Development* **13**, 3011–3053 (2020). <https://doi.org/10.5194/gmd-13-3011-2020>
- [15] M.D. Zelinka, T.A. Myers, D.T. McCoy, S. Po-Chedley, P.M. Caldwell, P. Ceppi, S.A. Klein, K.E. Taylor, Causes of Higher Climate Sensitivity in CMIP6 Models. *Geophysical Research Letters* **47**(1), 1–12 (2020). <https://doi.org/10.1029/2019GL085782>
- [16] D.J. Lunt, A. Farnsworth, C. Loptson, G.L. Foster, P. Markwick, C.L. Oapos Brien, R.D. Pancost, S.A. Robinson, N. Wrobel, Palaeogeographic controls on climate and proxy interpretation. *Climate of the Past* **12**(5), 1181–1198 (2016). URL <http://www.clim-past.net/12/1181/2016/cp-12-1181-2016-supplement.zippapers2://publication/doi/10.5194/cp-12-1181-2016-supplement>
- [17] Z. Sirkes, E. Tziperman, Identifying a damped oscillatory thermohaline mode in a general circulation model using an adjoint model. *Journal of Physical Oceanography* **31**(8 PART 2), 2297–2306 (2001). [https://doi.org/10.1175/1520-0485\(2001\)031<2297:iadotm>2.0.co;2](https://doi.org/10.1175/1520-0485(2001)031<2297:iadotm>2.0.co;2)
- [18] W. Weijer, H.A. Dijkstra, Multiple oscillatory modes of the global ocean circulation. *Journal of Physical Oceanography* **33**(11), 2197–2213 (2003). [https://doi.org/10.1175/1520-0485\(2003\)033<2197:MOMOTG>2.0.CO;2](https://doi.org/10.1175/1520-0485(2003)033<2197:MOMOTG>2.0.CO;2)
- [19] K.J. Meissner, M. Eby, A.J. Weaver, O.A. Saenko, CO₂ threshold for millennial-scale oscillations in the climate system: Implications for global warming scenarios. *Climate Dynamics* **30**(2-3), 161–174 (2008). <https://doi.org/10.1007/s00382-007-0279-0>
- [20] R.J. Haarsma, J.D. Opsteegh, F.M. Selten, X. Wang, Rapid transitions and ultra-low frequency behaviour in a 40 kyr integration with a coupled climate model of intermediate complexity. *Climate Dynamics* **17**(7), 559–570 (2001). <https://doi.org/10.1007/s003820000129>
- [21] E. Armstrong, K. Izumi, P. Valdes, Identifying the mechanisms of DO-scale oscillations in a GCM: a salt oscillator triggered by the Laurentide ice sheet. *Climate Dynamics* pp. 1–19 (2022)
- [22] P.J. Valdes, C.R. Scotese, D.J. Lunt, Deep ocean temperatures through time. *Climate of the Past* **17**(4), 1483–1506 (2021)
- [23] G. Vettoretti, P. Ditlevsen, M. Jochum, S.O. Rasmussen, Atmospheric co₂ control of spontaneous millennial-scale ice age climate oscillations. *Nature Geoscience* **15**(4), 300–306 (2022)
- [24] J. Chen, I.P. Montañez, S. Zhang, T.T. Isson, S.I. Macarewicz, N.J. Planavsky, F. Zhang, S. Rauzi, K. Daviau, L. Yao, et al., Marine anoxia linked to abrupt global warming during Earth’s penultimate icehouse. *Proceedings of the National Academy of Sciences* **119**(19), e2115231,119 (2022)
- [25] T.W. Wong Hearing, A. Pohl, M. Williams, Y. Donnadieu, T.H. Harvey, C.R. Scotese, P. Sepulchre, A. Franc, T.R. Vandenbroucke, Quantitative comparison of geological data and model simulations constrains early Cambrian geography and climate. *Nature Communications* **12**(1), 1–11 (2021)
- [26] R. Tostevin, B.J. Mills, Reconciling proxy records and models of Earth’s oxygenation during the Neoproterozoic and Palaeozoic. *Interface focus* **10**(June), 20190,137 (2020). <https://doi.org/10.1098/rsfs.2019.0137>
- [27] J. Alroy, M. Aberhan, D. Bottjer, M. Foote, F.T. Fürsich, P.J. Harries, A.J.W. Hendy, S.M. Holland, L.C. Ivany, W. Kiessling, M.A.

- Kosnik, C.R. Marshall, A.J. McGowan, A.I. Miller, T.D. Olszewski, M.E. Patzkowsky, S.E. Peters, L. Villier, P.J. Wagner, N. Bonusco, P.S. Borkow, B. Brenneis, M.E. Clapham, L.M. Fall, C.A. Ferguson, V.L. Hanson, A.Z. Krug, K.M. Layou, E.H. Leckey, S. Nürnberg, C.M. Powers, J.A. Sessa, C. Simpson, A. Tomasovych, C.C. Visaggi, Phanerozoic trends in the global diversity of marine invertebrates. *Science* **321**(5885), 97–100 (2008)
- [28] T.W. Dahl, M.L. Siggaard-Andersen, N.H. Schovsbo, D.O. Persson, S. Husted, I.W. Hougård, A.J. Dickson, K. Kjær, A.T. Nielsen, Brief oxygenation events in locally anoxic oceans during the Cambrian solves the animal breathing paradox. *Scientific Reports* **9**(1), 1–9 (2019). <https://doi.org/10.1038/s41598-019-48123-2>
- [29] J.L. Penn, C. Deutsch, J.L. Payne, E.A. Sperling, Temperature-dependent hypoxia explains biogeography and severity of end-Permian marine mass extinction. *Science* **362**(6419), eaat1327 (2018). URL <http://www.sciencemag.org/lookup/doi/10.1126/science.aat1327papers2://publication/doi/10.1016/j.cbpb.2017.12.017>
- [30] C. Deutsch, A. Ferrel, B. Seibel, H.O. Pörtner, R.B. Huey, Climate change tightens a metabolic constraint on marine habitats. *Science* **348**(6239), 1132–1136 (2015)
- [31] J.G. Rubalcaba, W.C. Verberk, A. Jan Hendriks, B. Saris, H. Arthur Woods, Oxygen limitation may affect the temperature and size dependence of metabolism in aquatic ectotherms. *Proceedings of the National Academy of Sciences of the United States of America* **117**(50), 31,963–31,968 (2020). <https://doi.org/10.1073/pnas.2003292117>
- [32] E. Tziperman, J.R. Toggweiler, Y. Feliks, K. Bryan, Instability of the thermohaline circulation with respect to mixed boundary conditions: Is it really a problem for realistic models? *Journal Of Physical Oceanography* **24**, 217–232 (1994)
- [33] P. Welander, A simple heat-salt oscillator. *Dyn. Atmos. Oceans* **6**, 233–242 (1982)
- [34] A. Colin de Verdière, A Simple Model of Millennial Oscillations of the Thermohaline Circulation. *Journal Of Physical Oceanography* **37**(5), 1142–1155 (2007)
- [35] A. Ridgwell, J.C. Hargreaves, N.R. Edwards, J.D. Annan, T.M. Lenton, R. Marsh, A. Yool, A. Watson, Marine geochemical data assimilation in an efficient Earth system model of global biogeochemical cycling. *Biogeosciences* **4**(1), 87–104 (2007). <https://doi.org/10.5194/bg-4-87-2007>
- [36] D. Ferreira, J. Marshall, J.M. Campin, Localization of deep water formation: Role of atmospheric moisture transport and geometrical constraints on ocean circulation. *Journal of Climate* **23**(6), 1456–1476 (2010). <https://doi.org/10.1175/2009JCLI3197.1>
- [37] P. Veervort, S. Kirtland Turner, F. Rochholz, A. Ridgwell, Earth System Model Analysis of How Astronomical Forcing Is Imprinted Onto the Marine Geological Record : The Role of the Inorganic (Carbonate) Carbon Cycle and Feedbacks. *Paleoceanography and Paleoclimatology* **36**, e2020PA004,090. (2021). <https://doi.org/10.1029/2020PA004090>
- [38] S.J.V.D. Velde, D. Hülse, C.T. Reinhard, A. Ridgwell, Iron and sulfur cycling in the cGENIE. muffin Earth system model (v0.9.21). *Geoscientific Model Development* **14**, 2713–2745 (2021)
- [39] L. Cao, M. Eby, A. Ridgwell, K. Caldeira, D. Archer, A. Ishida, F. Joos, K. Matsumoto, U. Mikolajewicz, A. Mouchet, J.C. Orr, G.K. Plattner, R. Schlitzer, K. Tokos, I. Totterdell, T. Tschumi, Y. Yamanaka, A. Yool, The role of ocean transport in the uptake of anthropogenic CO₂. *Biogeosciences* **6**(3), 375–390 (2009). <https://doi.org/10.5194/bg-6-375-2009>
- [40] S. Titz, T. Kuhlbrodt, S. Rahmstorf, U. Feudel, On freshwater-dependent bifurcations in box models of the interhemispheric thermohaline circulation. *Tellus A: Dynamic*

- Meteorology and Oceanography **54**(1), 89–98 (2002)
- [41] S. Titz, T. Kuhlbrodt, U. Feudel, Homoclinic bifurcation in an ocean circulation box model. *International Journal of Bifurcation and Chaos* **12**(04), 869–875 (2002)
- [42] K. Engelborghs, T. Luzyanina, G. Samaey, DDE-Biftool: a Matlab package for bifurcation analysis of delay differential equations. *TW Report* **305** (2000)
- [43] S.G. Janssens, On a normalization technique for codimension two bifurcations of equilibria of delay differential equations. Master’s thesis (2010)
- [44] J. Sieber, K. Engelborghs, T. Luzyanina, G. Samaey, D. Roose, DDE-BIFTOOL Manual — Bifurcation analysis of delay differential equations. *arXiv preprint arXiv:1406.7144* (2014)
- [45] B. Wage, Normal form computations for delay differential equations in DDE-Biftool. Master’s thesis (2014)
- [46] K. Pyragas, Continuous control of chaos by self-controlling feedback. *Physics letters A* **170**(6), 421–428 (1992)
- [47] S. Schikora, H. Wünsche, F. Henneberger, Odd-number theorem: Optical feedback control at a subcritical Hopf bifurcation in a semiconductor laser. *Physical Review E* **83**(2), 026,203 (2011)
- [48] A.S. Purewal, C.M. Postlethwaite, B. Krauskopf, Effect of delay mismatch in Pyragas feedback control. *Physical Review E* **90**(5), 052,905 (2014)
- [49] S.H. Strogatz, *Nonlinear dynamics and chaos with student solutions manual: With applications to physics, biology, chemistry, and engineering* (CRC press, 2018)
- [50] K.A. Crichton, A. Ridgwell, D.J. Lunt, A. Farnsworth, P.N. Pearson, Data-constrained assessment of ocean circulation changes since the middle Miocene in an Earth system model. *Climate of the Past* **17**(5), 2223–2254 (2021)
- [51] R. Marsh, A. Sobester, E.E. Hart, K. Oliver, N. Edwards, S. Cox, An optimally tuned ensemble of the “eb_go_gs” configuration of genie: parameter sensitivity and bifurcations in the Atlantic overturning circulation. *Geoscientific Model Development* **6**(5), 1729–1744 (2013)
- [52] R. Marsh, A. Yool, T. Lenton, M. Gulamali, N. Edwards, J. Shepherd, M. Krznaric, S. Newhouse, S. Cox, Bistability of the thermohaline circulation identified through comprehensive 2-parameter sweeps of an efficient climate model. *Climate Dynamics* **23**(7), 761–777 (2004)
- [53] C. Li, A. Born, Coupled atmosphere-ice-ocean dynamics in Dansgaard-Oeschger events. *Quaternary Science Reviews* **203**, 1–20 (2019)
- [54] A. Roberts, R. Saha, Relaxation oscillations in an idealized ocean circulation model. *Climate Dynamics* **48**(7), 2123–2134 (2017)
- [55] Z. Wang, L.A. Mysak, Glacial abrupt climate changes and Dansgaard-Oeschger oscillations in a coupled climate model. *Paleoceanography* **21**(2) (2006)
- [56] J.R. Shi, L.D. Talley, S.P. Xie, Q. Peng, W. Liu, Ocean warming and accelerating Southern Ocean zonal flow. *Nature Climate Change* pp. 1–8 (2021)
- [57] J.M.T. Thompson, J. Sieber, Predicting climate tipping as a noisy bifurcation: a review. *International Journal of Bifurcation and Chaos* **21**(02), 399–423 (2011)